Sparks and waves in a stochastic fire-diffuse-fire model of Ca^{2+} release

S. Coombes* and Y. Timofeeva†

Department of Mathematical Sciences, Loughborough University, Leicestershire, LE11 3TU, United Kingdom

(Received 24 January 2003; revised manuscript received 9 May 2003; published 25 August 2003)

Calcium ions are an important second messenger in living cells. Indeed, calcium signals in the form of waves have been the subject of much recent experimental interest. It is now well established that these waves are composed of elementary stochastic release events (calcium puffs or sparks) from spatially localized calcium stores. Here we develop a computationally inexpensive model of calcium release, based upon a stochastic generalization of the fire-diffuse-fire threshold model. Our model retains the discrete nature of calcium stores, but also incorporates a notion of release probability via the introduction of threshold noise. Numerical simulations of the model illustrate that stochastic calcium release leads to the spontaneous production of calcium sparks that may merge to form saltatory waves. In the parameter regime where deterministic waves exist, it is possible to identify a critical level of noise, defining a nonequilibrium phase transition between propagating and abortive structures. A statistical analysis shows that this transition is the same as for models in the directed percolation universality class. Moreover, in the regime where no initial structure can survive deterministically, threshold noise is shown to generate a form of array enhanced coherence resonance, whereby all calcium stores release periodically and simultaneously.

DOI: 10.1103/PhysRevE.68.021915 PACS number(s): 87.10.+e, 87.17.−d

I. INTRODUCTION

Variations in calcium concentrations are a vital component of many cellular processes, including intracellular and extracellular signaling processes, muscle contraction, cell fertilization, cell aptoptosis, and neuronal plasticity [1]. Innovative techniques for calcium imaging have allowed experimentalists to resolve spatiotemporal patterns of oscillations and waves in both isolated cells and tissue (see, for example, Ref. [2]). These dynamical phenomena are believed to be subserved by specific molecular mechanisms for the control of calcium influx and efflux through the cell's outer membrane. This is typically effected by voltage-gated ion channels, calcium exchangers and pumps, as well as calcium release mechanisms from internal compartments within the sarcoplasmic or endoplasmic reticulum and mitochondrial stores (see Ref. [3] for a tutorial discussion). When calcium is released from internal stores into the cytosol, a wave of increased concentration can travel without deformation, defining smooth propagation, or with a lurching quality, defining saltatory propagation. For example, the calcium release wave in immature xenopus oocytes is saltatory while the fertilization wave in mature oocytes is smooth. There is a vast and growing body of theoretical work devoted to understanding the basic biophysical mechanisms underlying these waves (see, for example, Refs. [4–6]). A common starting point for much of this work is the observation that Ca^{2+} is released from internal stores through channels with nonlinear properties. A form of autocatalytic amplification, known as calcium-induced-calcium-release, favors channel opening in the presence of increased cytosolic calcium. After an open channel closes via inactivation, it cannot reopen for some time during which it is in a *refractory* state. Thus, the release of Ca^{2+} by intracellular stores is self-regulating. A variety of kinetic schemes have been proposed in connection with these mechanisms and typically lead to deterministic models which reduce to either excitable, oscillatory, or bistable dynamical systems. If whole cell models are assumed to be of reaction diffusion type then powerful techniques from continuum mechanics can be brought to bear in studying nonlinear waves [7–14]. When models respect the fact that channels act as discrete Ca^{2+} stores, translation symmetry is broken and one cannot use such techniques. Importantly, this loss of translation symmetry is a prerequisite for the existence of a saltatory wave. However, the observation of spontaneous Ca^{2+} puffs or sparks and the fact that calcium waves can abort suggest that a predominantly deterministic model, whether based on a discrete or continuum description of stores, is still not the whole story. Keizer and Smith [15] and Falcke, Isimring, and Levine [16] have emphasized the importance of modeling stochastic release kinetics when considering initiation and subsequent propagation of waves. Both have observed waves that abort in the presence of noise, and also shown how noise may generate a spark-to-wave transition. A recent numerical study of the spark-to-wave transition in cardiac cells may be found in Ref. [17].

The model of Keizer and Smith considers a stochastic ryanodine receptor channel embedded with a continuous cell model of reaction diffusion type. The numerical simulation of the model requires combining the evolution of a nonlinear partial differentiation equation (PDE) with a continuous time Markov process describing the transitions between the open, closed, and several intermediate states of the ryanodine receptor. The model of Falcke, Isimring, and Levine considers a stochastic version of the De Young–Keizer inositol 1,4,5-trisphosphate (IP_3) receptor model, but with channel clusters at lattice points coupled by *fast* diffusion. The assumption of fast diffusion and linearity of the equation for calcium transport allows an adiabatic elimination of the calcium dynamics in favor of purely stochastic continuous time Markov process

*Electronic address: S.Coombes@lboro.ac.uk
†Electronic address: I.Timofeeva@lboro.ac.uk

for the channel configurations of the IP_3 receptor. Without the need to numerically evolve a PDE to determine calcium profiles, this leads to a computationally cheap model.

In this paper we will pursue the construction of another computationally cheap, yet biophysically realistic, model of intracellular calcium release. We take as our starting point the deterministic fire-diffuse-fire (FDF) model of Keizer *et al.* [18]. This was originally intended as a model of cardiac myocytes, in which calcium release occurs via ryanodine receptor Ca^{2+} channels located in a regular array in the sarcoplasmic reticulum. However, the model can also be formulated for a continuum distribution of stores [19]. Moreover, a version of the FDF model, which describes IP_3 receptors, has recently been introduced, motivated by a reduction of the De Young–Keizer model [14]. A mathematical analysis of waves in the deterministic FDF model can be found in Refs. [19–22]. The FDF model uses a threshold process to mimic the nonlinear properties of Ca^{2+} channels. A stochastic generalization of the model is introduced after considering how threshold noise can determine release probability. Functional forms for the distribution of this threshold noise can be inferred from the recent observation of Izu, Wier, and Balke [17] that the probability of release per unit time has a sigmoidal functional form. This leads to a model with simple probabilistic update rules for the release of calcium from internal stores. By avoiding a Markov process description of channel gating, we sidestep the need for computationally expensive Monte Carlo–type simulations. Moreover, the simplicity of the underlying deterministic FDF model can lead to further computational improvements. When considering a discrete set of release sites and calcium puffs that have a simple on/off temporal structure, the calcium profile can be solved for in closed form, without the need for assumptions such as fast diffusion. This obviates the need to numerically evolve a PDE to obtain calcium profiles.

In Sec. II we describe the FDF model with a discrete distribution of release sites. We prefer to discuss the discrete rather than the continuous formulation of the model since it is less studied, yet reduces to the continuum description in the limit of zero spacing between release sites. We make the assumption that release events occur on a regular temporal lattice, to simplify the model so that it may be rewritten in the language of binary *release events*. As it stands, the original FDF model does not allow for any refractory processes. We introduce a dynamics for the release events, which also serves as a simple phenomenological model for refractoriness. The calcium profile of the model can then be written as the the sum of two terms. The first is a linear combination of basis functions, with coefficients given by the release events. The second is a simple convolution of the initial data with the Green's function of the model without stores. In this deterministic model, release events are calculated via a thresholding of the calcium profile at a release site. Direct numerical simulations are used to show that this computationally simple version of the FDF model provides an accurate representation of the original. Moreover, it is in the ideal form to be generalized to incorporate stochastic effects. The FDF threshold is assumed to be the most appropriate point at which to introduce a source of noise to the model. We show how this leads to a natural description of release events, using a probabilistic rather than a deterministic update rule. The effects of threshold noise are explored in Sec. III. Here, we focus on a one-dimensional cell model that, in the absence of noise, can support a traveling saltatory wave. Sufficiently large threshold noise is able to terminate a wave prematurely, suggesting that for some critical noise level, there is a nonequilibrium phase transition between propagating and abortive waves. A statistical analysis shows that the model exhibits properties consistent with the behavior of other models from the universality class of directed percolation (see Ref. [23] for a review). A study of a two-dimensional cell model is presented in Sec. IV. Here, we show that not only does the model support noisy circular and spiral waves, as expected, but can also exhibit a form of array enhanced coherence resonance [24–26]. We find that coherent motion, in the form of simultaneous and periodic release of calcium from all stores can be induced purely by noise. Finally, in Sec. V we discuss natural generalizations of our model.

II. THE MODEL

The FDF model [18–22] is an idealized model of Ca^{2+} release from internal stores in living cells. It is an all or nothing release model in which a fixed amount of Ca^{2+} is released when the cytosolic Ca^{2+} density in the neighborhood of a release site reaches a certain threshold. The partial differential equation describing the density of Ca^{2+}, denoted by $u(\mathbf{r},t)$, is given by

$$\frac{\partial u}{\partial t} = -\frac{u}{\tau_d} + D\nabla^2 u + \sum_{n\in\Gamma}\sum_{m\in\mathbb{Z}} \delta(\mathbf{r}-\mathbf{r}_n)\,\eta(t-T_n^m) \quad (1)$$

with $\mathbf{r}\in\mathbb{R}^l$ and $t\in\mathbb{R}^+$. Here, l is the physical dimension of the cell model and Γ is a discrete set that indexes the stores. Vectors $\mathbf{r}_n$ determine the locations of the (point) Ca^{2+} release sites, whilst the T_n^m give the time of release of the mth puff at the nth release site. The function $\eta(t)$ describes the shape of a Ca^{2+} puff, which we shall take to be a rectangular pulse shape given by

$$\eta(t) = \frac{\sigma}{\tau}\Theta(t)\Theta(\tau-t), \quad (2)$$

where Θ is a Heaviside step function. The strength of the calcium puff is σ, and τ is interpreted as the rise time of the receptor. The model is highly nonlinear because the release events are implicitly determined by the times at which the Ca^{2+} density at a release site takes the threshold value u_c. More precisely, we write

$$T_n^m = \inf\{t | u(\mathbf{r}_n,t) > u_c, u_t(\mathbf{r}_n,t) > 0, T_n^m > T_n^{m-1} + \tau_R\}, \quad (3)$$

to indicate that release events must be separated by at least a time τ_R, the refractory time scale. The decay time τ_d in Eq. (1) models the time scale associated with the action of sarcophasmic/endoplasmic reticulum calcium pumps that resequester the Ca^{2+} back into the stores. The transport of

Ca^{2+} is assumed to be by diffusion with diffusion coefficient D. The mode of propagation (continuous or saltatory) depends on the ratio of the time that a single site remains open to the time it takes for calcium to diffuse between neighboring release sites [19]. If this ratio is large enough, the propagation is continuous and wave speeds scale as $\sqrt{D}$, and if it is small enough the propagation is saltatory and wave speeds scale linearly with D. The analytical tractability of the model is not only useful for gaining insight into the dependence of wave speed on system parameters, but can help in reducing the computational demands on a numerical scheme for the self-consistent evolution of Eq. (1). Consider for the moment, the class of solutions where all release times occur at integer multiples of τ. In this case, we may write

$$\sum_m \eta(T_n^m) = \sum_p \eta(p\tau) a_n(p) \tag{4}$$

for all n, where we define the *release function* $a_n(p)$ as

$$a_n(p) = \begin{cases} 1 & T_n^m = p\tau \\ 0 & \text{otherwise.} \end{cases} \tag{5}$$

In general, the release times will not occur at multiples of τ. However, by restricting the system so that release times do occur on a regular temporal lattice, and choosing $\tau_R = R\tau$ for some $R \in \mathbb{Z}$, we may write

$$a_n(p) = \Theta(u_n(p) - u_c) \prod_{m=1}^{\min(R,p)} \Theta(u_c - u_n(p-m)), \tag{6}$$

where $u_n(p) \equiv u(\mathbf{r}_n, p\tau)$. The first term on the right hand side is a simple threshold condition for the determination of a release event while the second term ensures that release events are separated by at least τ_R. This restriction of the model eliminates the need for the precise determination of release times. The FDF model then takes the particularly simple form

$$Qu(\mathbf{r},t) = \frac{\sigma}{\tau} \sum_{n\in\Gamma} a_n(p)\, \delta(\mathbf{r}-\mathbf{r}_n), \quad p\tau < t < (p+1)\tau, \tag{7}$$

where Q is the linear differential operator

$$Q = \partial_t + \frac{1}{\tau_d} - D\nabla^2, \tag{8}$$

with Green's function

$$G(\mathbf{r},t) = [4\pi D t]^{-l/2} \exp\left(-\frac{t}{\tau_d}\right) \exp\left(-\frac{r^2}{4Dt}\right), \tag{9}$$

and $r = |\mathbf{r}|$. The dynamics for $p\tau < t < (p+1)\tau$ is completely determined in terms of initial data $u_p(\mathbf{r}) = u(\mathbf{r}, p\tau)$ as

$$u(\mathbf{r},t) = \frac{\sigma}{\tau} \sum_{n\in\Gamma} a_n(p) H(\mathbf{r}-\mathbf{r}_n, t-p\tau) + (G \otimes u_p)(\mathbf{r},t), \tag{10}$$

where

$$H(\mathbf{r},t) = \int_0^t G(\mathbf{r}, t-s)\, ds \tag{11}$$

and

$$(G \otimes u_p)(\mathbf{r},t) = \int_{\mathbb{R}^l} G(\mathbf{r}-\mathbf{r}', t-p\tau) u_p(\mathbf{r}')\, d\mathbf{r}'. \tag{12}$$

Compared to the original FDF model, the one we have described here is computationally cheaper to solve. Release events defined by $a_n(p) = 1$ are easily calculated since $u_n(p) \equiv u_p(\mathbf{r}_n)$ may be written as a sum of two terms that are both amenable to fast numerical evaluation. In particular, $u_p(\mathbf{r})$ may be written in terms of the *basis* functions $H_n(\mathbf{r}) = \sigma H(\mathbf{r}-\mathbf{r}_n, \tau)/\tau$, so that

$$u_p(\mathbf{r}) = \sum_{n\in\Gamma} a_n(p-1) H_n(\mathbf{r}) + (G \otimes u_{p-1})(\mathbf{r}, p\tau). \tag{13}$$

Since the basis functions $H_n(\mathbf{r})$ are fixed for all time, they need only be computed once. For small τ we also have the useful result that $H(\mathbf{r},\tau) \to G(\mathbf{r},\tau)$, which is given in closed form by Eq. (9). The convolution in Eq. (13) may be performed efficiently using fast Fourier transform (FFT) techniques. Once again the FFT of $G(\mathbf{r},\tau)$ need only be computed once, so that it is only necessary to successively construct the FFT of $u_p(\mathbf{r})$ for $p = 0,1,2, \ldots$. We then have that $G \otimes u_p = \mathcal{F}^{-1}(\mathcal{F}[G]\mathcal{F}[u_p])$, where $\mathcal{F}$ denotes the FFT. Hence, under the assumption that release times occur on some regular temporal lattice, the model does not have to be evolved as a discontinuous PDE with a self-consistent search for the times of threshold crossings that define release events.

Of course, the above approach is only useful if the restricted class of solutions that we have focused on is, in some sense, close to solutions of the full model. To illustrate that this is the case for practical applications, we consider a one-dimensional cell with a regular spacing of release sites. The exact solution of a saltatory traveling pulse to this model, given by Coombes [22], provides a benchmark against which to test our reduction of the FDF model. We denote position within the cell by x and place release sites at points $x_n = nd$, where d is the release site spacing. In one dimension, $H(x,t)$ is available in closed form [22] as $H(x,t) = A(x,0) - A(x,t)$, where

$$A(x,t) = \frac{1}{4}\sqrt{\frac{\tau_d}{D}}\left[\exp\left(\frac{-|x|}{\sqrt{\tau_d D}}\right) \operatorname{erfc}\left(-\frac{|x|}{\sqrt{4Dt}} + \sqrt{\frac{t}{\tau_d}}\right) + \exp\left(\frac{|x|}{\sqrt{\tau_d D}}\right) \operatorname{erfc}\left(\frac{|x|}{\sqrt{4Dt}} + \sqrt{\frac{t}{\tau_d}}\right)\right]. \tag{14}$$

In Fig. 1 we plot the speed of a lurching solitary pulse as given in Ref. [22] for the full FDF model. In the same figure, we plot numerical results obtained from our reduced FDF model. It can be seen that there is an excellent agreement between the two, justifying the practical assumption that release events can be considered to occur only at integer mul-

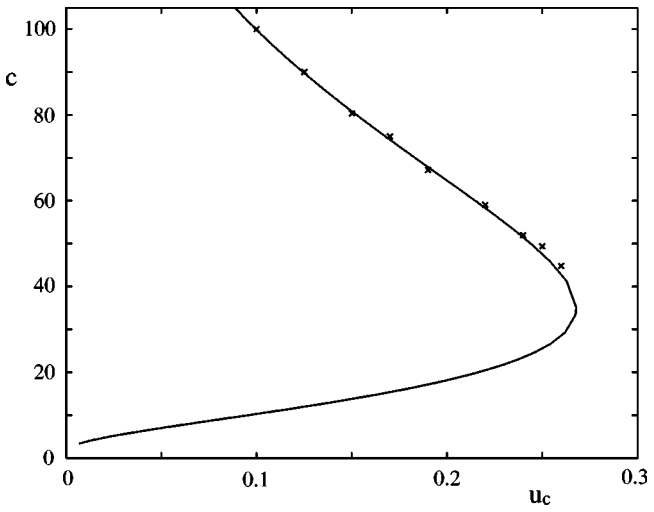

FIG. 1. Speed of a solitary pulse as a function of the threshold level u_c in the FDF model. Crosses denote results from simulations of the reduced FDF model with 500 regularly spaced stores. Parameters: $d=2$ μm, $D=30$ μm^2/s, $\tau=10$ ms, and $\tau_d=0.2$ μM/s.

tiples of the calcium puff duration. From experimental data it is apparent that the refractory time scale is typically 50 times that of the release duration (see Ref. [15] for a discussion), so we take $R=50$. Typically, τ is approximately 10–20 ms [27].

Stochastic model

Release sites are typically composed of clusters whose size (typically between 10 and 100 channels) is a key parameter determining the fluctuations in mean open probability of release (see Ref. [28] for a recent discussion). Here, we consider the stochastic gating of receptor channels to give rise to an effective threshold that can be modeled under the replacement $u_c \to u_c+\xi$, where ξ is an additive noise term with distribution $\rho(\xi)$. The probability that $a_n(p)=1$ is then given by

$$P(a_n(p)=1)=P(u_n(p)>u_c)\prod_{m=1}^{\min(R,p)} P(u_n(p-m)<u_c), \tag{15}$$

where

$$P(u>u_c)=\int \rho(\xi)\Theta(u-u_c-\xi)d\xi. \tag{16}$$

For convenience, we choose $\rho(\xi)=f'(\xi)$ so that

$$P(u>u_c)=f(u-u_c). \tag{17}$$

In the work by Izu, Wier, and Balke [17] it has been argued that the probability of release per unit time follows a functional form given by $u^n/(K^n+u^n)$, with the Hill coefficient $n=1.6$ and Ca^{2+} sensitivity parameter $K=15$ μM. This suggests that natural choices for $f(\xi)$ are sigmoidal functions. Here, we shall make the choice

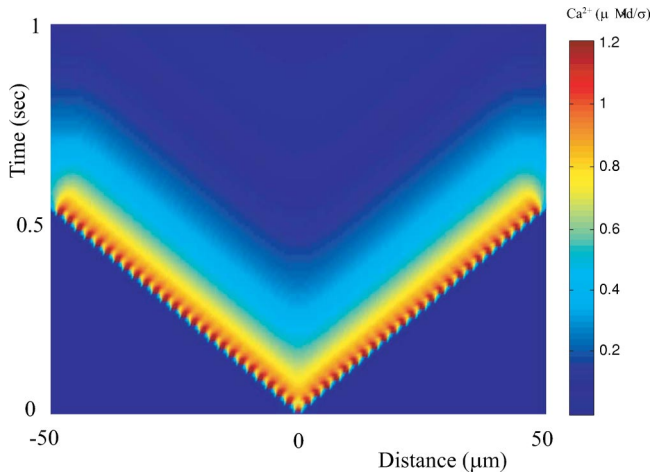

FIG. 2. (Color online) An example of two lurching pulses moving out from the center of a deterministic one-dimensional FDF model with 50 regularly spaced release sites and free boundary conditions. Parameters are as in Fig. 1, for a cell of linear dimension 100 μm and $u_c=0.1$.

$$f(\xi)=\left\{\frac{1}{1+e^{-\beta\xi}}-\frac{1}{1+e^{\beta u_c}}\right\}(1+e^{-\beta u_c}), \tag{18}$$

so that the probability of release is zero when $u=0$ and tends to one as $u\to\infty$. In summary, the stochastic FDF model is defined by Eq. (10) with the $a_n(p)\in\{0,1\}$ treated as random variables, such that $P(a=1)$ is given by Eq. (15). In this framework, the refractory time scale can also be thought of as being drawn from some distribution, since release events are no longer bound by the constraint that they be separated by at least τ_R. In the limit $\beta\to\infty$, $f(\xi)$ approaches a step function so that $P(u>u_c)=\Theta(u-u_c)$ and we recover our original deterministic model. Thus, we interpret β as a parameter describing the level of noise. Note that for sigmoidal forms of f, the noise distribution $\rho=f'$ is bell shaped with the width of the bell controlled by β.

To illustrate the sort of behaviors that can be generated by this stochastic model, we again turn to a one-dimensional cell model with regularly spaced release sites. We begin all our simulations with an initial release site in the middle of the cell in an open state. A space-time density plot of a solitary lurching pulse, arising in the deterministic limit $\beta\to\infty$, is shown in Fig. 2. This is useful as a starting point for comparison with results from the stochastic model, and nicely illustrates that a discrete set of release sites leads to a wave that propagates with a nonconstant profile, but with a well defined speed. In Fig. 3 we plot the corresponding behavior in the presence of a finite amount of noise. Initial release from the central site leads to a local elevation of Ca^{2+}, which initiates a propagating Ca^{2+} wave via activation of nearby sites, as in the deterministic case. However, the stochastic nature of the wave is evident from the fact that it does not propagate symmetrically away from the initial event. Although rather well defined to start with, the leftward propagating wave terminates at around 1.4 s. Activity in the wake of the primary stochastic front can also be sufficient to

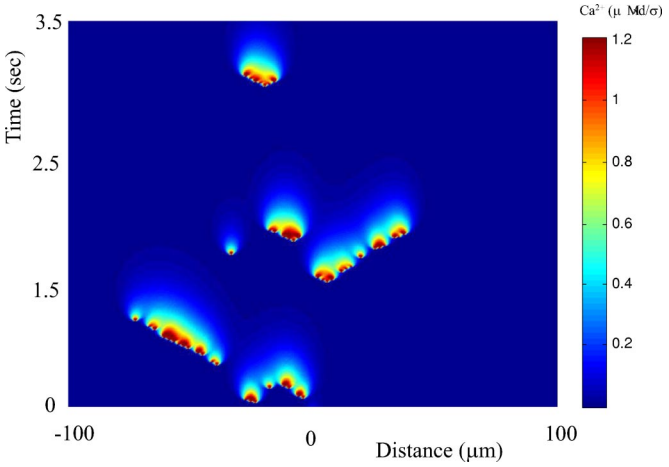

FIG. 3. (Color online) Stochastic traveling wave for the model of Fig. 2, with a finite amount of noise. Here, $\beta=10$.

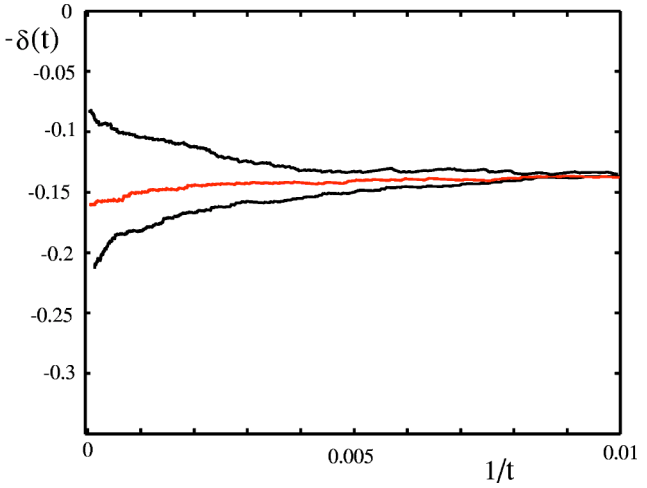

FIG. 4. (Color online) A plot of $-\delta(t)$ as a function of t^{-1} for three different level of threshold noise, $\beta=0.49$ (upper curve), $\beta=0.47$ (middle curve), and $\beta=0.45$ (lower curve).

prime release sites for subsequent spark production, seen at around 1.6 s and again at around 3.2 s. It is also possible for propagating pulses to lead to the creation (in their wake) of oppositely propagating pulses. This so-called *back firing* has been observed in a number of models (see, for example, Refs. [29,30]), including the stochastic calcium release models of Keizer and Smith [15] and Falcke [16]. Note that it is also possible for spontaneous sparks to recruit enough neighbors for the initiation of a stochastic front. In the following section, we consider in more detail the statistical properties of FDF waves in the presence of threshold noise.

III. DIRECTED PERCOLATION

From Fig. 1 it is easy to see that the deterministic FDF model can support traveling waves if the threshold for release is not too high, i.e., if $u_c<u_c^*$, where u_c^* is defined by the saddle-node bifurcation where the fast and slow branches of $c=c(u_c)$ coalesce. However, in the regime where $u_c<u_c^*$, it is possible that noisy versions of these waves will fail to propagate if noise levels are too high. This leads to the interesting possibility of a critical noise that define a border between waves which *survive* or eventually go *extinct*. Indeed, Bär *at al.* [31] have produced numerical evidence that the model of Falcke *et al.* exhibits a nonequilibrium phase transition belonging to the so-called directed percolation (DP) universality class. DP is the new testing ground of nonequilibrium statistical mechanics, much as the Ising model is for equilibrium statistical physics. The analysis of the DP universality class is highly nontrivial and it has only been possible to obtain critical exponents for models in this class numerically. Precisely at the critical point, the survival probability $\Pi(t)$ of a wave is expected to scale asymptotically as $t^{-\delta}$ (see Ref. [23] for a review). The best current estimate for δ comes from the work of Jensen [32], who finds that $\delta\sim0.159\,464$. According to the Janssen-Grassberger DP conjecture, any spatiotemporal stochastic process with short range interactions, fluctuating active phase and unique nonfluctuating (absorbing) state, single order parameter, and no additional symmetries, should belong to the DP class. Since these are almost the defining characteristics of a minimal model for stochastic calcium release, we should not be too surprised if our stochastic FDF model also belongs to the DP class. To explore this possibility we consider the behavior of our model under variation of the noise parameter β. We denote the critical value of β at the phase transition between propagating and abortive waves by β_c. To obtain a good estimate of the critical exponent δ, we construct the following effective exponent:

$$\delta(t)=\frac{\ln[\Pi(rt)/\Pi(t)]}{\ln r}, \tag{19}$$

where $\ln r$ is the distance used for estimating the slope of $\Pi(t)$. For $\beta\neq\beta_c$, $\delta(t)$ will deviate from a straight line (in the large t limit) so that plots of $\delta(t)$ for various choices of β may be used to predict β_c. An estimate of δ is obtained by extrapolating the behavior of $\delta(t)$ to $t^{-1}=0$. In Fig. 4 we plot $\delta(t)$ for various β, showing that for our choice of system parameters, $\beta_c\sim0.47$. In Fig. 5 we plot the corresponding distribution of survival times $\Pi(t)$ for the activation process started from a single site. Using our value of β_c we find $\delta\sim0.159$, suggesting that our model does indeed belong to the DP universality class. Whether or not a DP transition will be seen in a living cell is another matter entirely. As pointed out by Hinrichsen [23], the size of a living cell is only a few orders of magnitude larger than the diffusion length, leading to strong finite size effects. Moreover, inhomogeneities as well as internal cellular structures are a source of disorder that may further complicate matters. To date, there is no clear experimental evidence that there is a phase transition between survival and extinction of propagating calcium waves in living cells.

Up to now, we have illustrated the properties of the stochastic FDF model with one-dimensional studies in the regime where wave propagation is possible in the limit of zero threshold noise. In the following section, we turn to two-

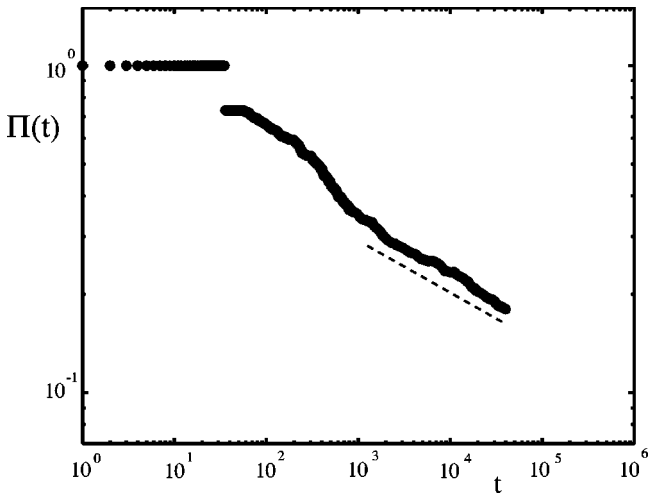

FIG. 5. The distribution of survival times for the stochastic FDF model at the critical noise defining the transition between propagating and abortive waves. For large t, $\Pi(t)$ scales as $t^{-0.159}$, indicating that our model belongs to the DP universality class.

dimensional studies and also explore the parameter regime where an initial disturbance could not propagate in the deterministic regime.

IV. ARRAY ENHANCED COHERENCE RESONANCE

In this section, we consider a two-dimensional cell model and a regular square lattice of release sites with spacing d. The basis functions $H(\mathbf{r}-\mathbf{r}_n)$ can be computed numerically from Eqs. (11) and (9), using $l=2$. However, it is also possible to compute the basis functions in closed form for two special cases.

(i) In the limit $\tau_d \to \infty$, $H(\mathbf{r})=E_1(r^2/4D\tau)/4\pi D$, where $E_1(x)$ is the exponential integral function

$$E_1(x)=\int_x^\infty dz \frac{e^{-z}}{z}. \tag{20}$$

This corresponds to the limit of zero pumping, where calcium is not removed from the cytosol.

(ii) For small τ, we also have that $H(\mathbf{r},\tau)\to G(\mathbf{r},\tau)$ (as already noted in Sec. II). Since the puff duration is very small compared to τ_R, this is a very accurate approximation and so, has been used in numerical simulations for this section.

An example of behavior in the two-dimensional stochastic FDF model is shown in Fig. 6. Here, a sequence of snap shots shows nucleation of a circular front, subsequent propagation, and the emergence of noisy spiral waves. These waves can be annihilated in collisions with other waves and created by spontaneous nucleation. The long time behavior of the system is dominated by the interaction of irregular target and spiral waves. This is typical of dynamics in noisy spatially extended excitable systems. In fact, the role of fluctuations for the generation and propagation of patterns in spatially extended excitable media is a subject of increasing attention and can be traced back to work by Jung and Mayer-Kress [33,34]. We note that both the stochastic FDF model

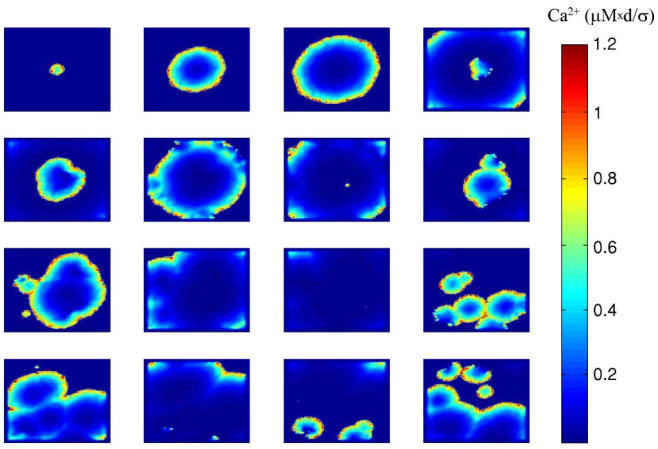

FIG. 6. (Color online) Temporal sequence snapshots for the two-dimensional stochastic FDF model with $\beta=100$ (low noise). Other parameters are as in Fig. 1. Frames are presented every 0.45 s, starting in the top left corner and moving rightward and down. An initial seed in the center of the cell model leads to the formation and propagation of a circular front. Spiral waves form in the wake of the wave by spontaneous nucleation. These can be destroyed in wave-wave collisions and created by spontaneous nucleation.

and the Jung and Mayer-Kress (JMK) model describe the interaction of threshold devices with spatially decaying connectivity (fixed in the JMK model, but determined by the calcium profile in ours). In the JMK model, noise is added to the state variable whereas in the stochastic FDF model it is added to the threshold. Importantly, it is possible for noise to sustain spatiotemporal structures that could not otherwise occur. In this case, a removal of all noise would lead to a deterministic system which could not support traveling waves. Since noise sustained target waves may collide with each other, this typically limits their growth to a finite region, whose size is expected to decrease with increasing noise. Indeed, the scale of noisy spiral waves has been shown to be dominated by the ratio of longitudinal (normal to the front of high activity) and the traversal (parallel to the front) speed of propagation [33]. As noise levels increase, the transversal propagation speeds up, yielding a spiral wave with larger curvature. For increasing noise, it is possible that the breakup of spirals and increased spontaneous nucleation of other spirals may destroy any coherent motion. However, it is also possible to see coherent motion for high levels of noise. In fact, coherence can actually be enhanced in regions of high noise and it is possible to observe synchronized global release events. This type of behavior has recently been termed *array enhanced coherence resonance* (AECR) and is typical of the way in which noise can lead to structured activity in spatially extended excitable systems [24–26]. In Fig. 7 we show an example of this type of phenomenon in the stochastic FDF model. Here, an initial disturbance leads to the propagation of a circular target wave. In the wake of the wave, there is a subsequent release from a set of neighboring sites. After this, one sees near simultaneous release from a large number of sites. This process of simultaneous release repeats, and at every stage recruits more and more stores. After only a few cycles of this process one sees an almost simultaneous release from all sites. This causes an oscillation

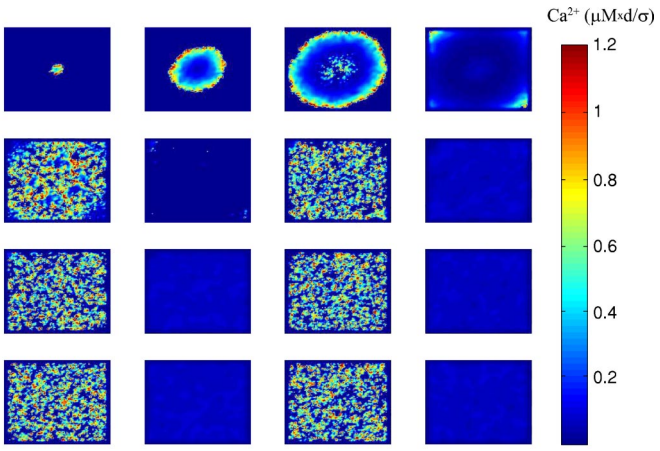

FIG. 7. (Color online) Temporal sequence snapshots for the two-dimensional stochastic FDF model with $\beta=10$ (high noise). Other parameters are as in Fig. 1. Frames are presented every 0.45 s, starting in the top left corner and moving rightward and down. An initial seed leads to the formation of a circular traveling front. In the wake of the wave, there is periodic and near simultaneous release from a large number of stores, typical of systems exhibiting array enhanced coherence resonance.

in the global signal $U(t)$, defined by

$$U(t)=\frac{1}{|\Gamma|}\sum_{n=1}^{|\Gamma|}u(\mathbf{r}_n,t), \tag{21}$$

where $|\Gamma|$ is the number of release sites. An example of this oscillation is shown in Fig. 8 for the data of Fig. 7. In this figure, we also plot the variation of $U(t)$ for the data presented in Fig. 6. Although showing some level of periodic behavior, it is clearly not as regular as that of the AECR example. The frequency of the AECR oscillation [as measured by variation in $U(t)$] increases monotonically with the noise level β^{-1} (above a cutoff below which AECR fails), and is shown in Fig. 9. We emphasize that the coherent motion illustrated in Fig. 7 is induced purely by noise, without

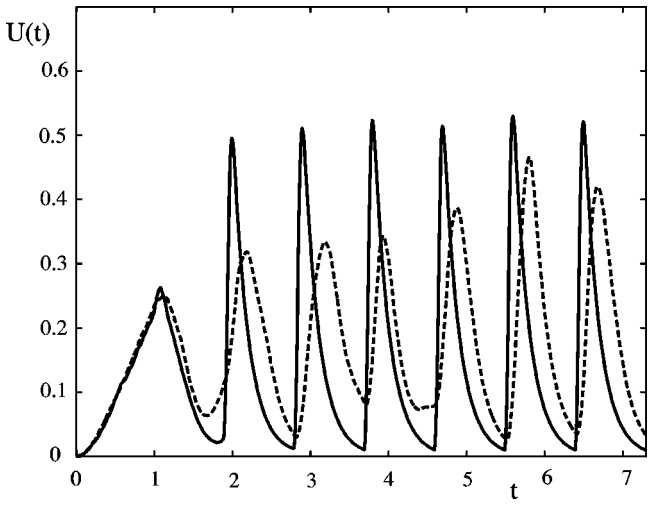

FIG. 8. Plot of the global signal $U(t)$ for the data of Fig. 7 (solid line) and also that of Fig. 6 (dashed line).

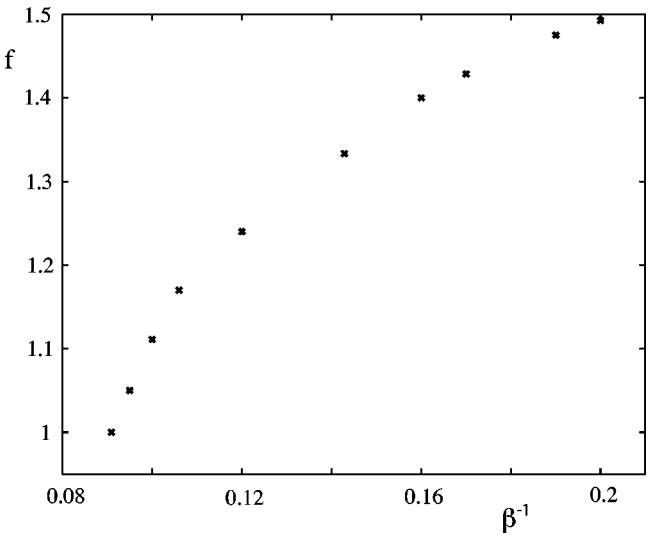

FIG. 9. Frequency f of oscillation of $U(t)$ for the system exhibiting array enhanced coherence resonance, as a function of β^{-1}. Note that frequency increases monotonically with increasing noise levels. Parameters are as in Fig. 7.

an external periodic signal. This is very reminiscent of the behavior of an excitable activator-inhibitor medium recently discussed by Hempel, Schimansky-Geier, and Garcia-Ojalvo [24]. They also consider a model with threshold noise (but with fixed Gaussian spatial interactions) and note that when the nucleation time becomes much smaller than the intrinsic refractory time of the system, all cells fire and come back to rest essentially at the same time.

V. DISCUSSION

In this paper we have introduced a stochastic generalization of the fire-diffuse-fire model of calcium release from internal stores in single cells. This computationally inexpensive model has been numerically simulated in one and two dimensions. The model exhibits a nonequilibrium phase transition between propagating and nonpropagating waves of the type seen in models belonging to the directed percolation universality class. Moreover, noise sustained patterns can give way to a form of array enhanced coherence resonance with increasing levels of threshold noise. A number of natural extensions of the model are possible, which we now briefly discuss.

In a recent paper, we have shown that the biophysically motivated De Young–Keizer model [35] of calcium release can be viewed as possessing an IP_3 sensitive threshold [14]. The use of this IP_3 sensitive threshold within the stochastic FDF framework would allow the investigation of the effects of stochastic fluctuations in IP_3 levels in models of De Young–Keizer type. Although not expected to influence any critical exponents (since these should be independent of the details of the model), the background level of IP_3 would be expected to influence the speed and shape of a traveling wave. Interestingly, precisely this issue has been recently addressed by Shuai and Jung [36] in a model of Ca^{2+} release, which incorporates a stochastic model of an IP_3 receptor.

In real cells, release sites are not likely to be arranged on a perfectly regular lattice (although for cardiac myocytes, release sites are in fact regularly spaced along the longitudinal axis of the cell) and one should consider a disordered distribution of sites. A numerical investigation of the effects of spatial disorder on models of calcium release has suggested that the propagation of waves in a cell with randomly distributed release sites is reminiscent of that seen in forest fire models, flame propagation in random materials, and epidemic spread [37,38]. Similar studies of the computationally cheap stochastic FDF model will allow a comprehensive statistical analysis, useful for uncovering the criterion for wave propagation as a function of spatial disorder. Although we have focused on regular distributions of release sites for the purposes of this paper, there is no computational overhead in considering disordered distributions of stores.

Throughout this paper we have made the assumption that diffusion is isotropic. The relaxation of this assumption does not lead to any technical difficulties. For example, in two dimensions we might consider the replacement $D\nabla^2 \to D_x\partial_{xx}+D_y\partial_{yy}$, so that $G(x,y,t) = \exp[-t/\tau_d]\exp[-x^2/4D_xt-y^2/4D_yt]/4\pi\sqrt{D_xD_y}t$. The remainder of the formalism we have employed then carries over.

By combining the above generalizations of the model it will also be possible to explore the importance of *focal sites* on wave initiation and propagation. Focal release sites are distinguished by their higher sensitivity to IP_3 and their close apposition to neighboring release sites. They are known to be able to entrain both the temporal frequency and spatial directionality of calcium waves [39]. Interestingly, this issue has recently been considered by Falcke from a theoretical perspective [40,41]. Falcke shows that for a stochastic realization of the De Young–Keizer model, large period (noise induced) oscillations may be perceived as a nucleation phenomena where the period of oscillation depends on the geometry of the array of release sites.

All these generalizations, together with fully three-dimensional simulations, are topics of current investigation.

ACKNOWLEDGMENTS

We would like to thank Mike Kearney for stimulating discussions about the physics of directed percolation.

[1] M.J. Berridge, J. Neurophysiol. **499**, 291 (1997).
[2] *Calcium Signaling (Methods in Signal Transduction)*, edited by J.W. Putney (CRC Press, London, 1999).
[3] B. Alberts, A. Johnson, J. Lewis, M. Raff, K. Roberts, and P. Walter, *Molecular Biology of the Cell* (Garland Science, New York, 2002).
[4] A. Goldbeter, *Biochemical Oscillations and Cellular Rhythms* (Cambridge University Press, Cambridge, 1996).
[5] J. Keener and J. Sneyd, *Mathematical Physiology* (Springer, New York, 1998).
[6] *Computational Cell Biology*, edited by C.P. Fall, E.S. Marland, J.M. Wagner, and J.J. Tyson (Springer, New York, 2002).
[7] J. Sneyd, S. Girard, and D. Clapham, Bull. Math. Biol. **55**, 315 (1993).
[8] G. DuPont and A. Goldbeter, Biophys. J. **67**, 2191 (1994).
[9] J. Sneyd, J. Keizer, and M.J. Sanderson, FASEB J. **9**, 1463 (1995).
[10] M.S. Jafri and J. Keizer, Bull. Math. Biol. **59**, 1125 (1997).
[11] J. Sneyd, P.D. Dale, and A. Duffy, SIAM (Soc. Ind. Appl. Math.) J. Appl. Math. **58**, 1178 (1998).
[12] G.C. Chopra, B.D. Sleeman, J. Brindley, D.G. Knapp, and A.V. Holden, Bull. Math. Biol. **61**, 273 (1999).
[13] J. Sneyd, A. LeBeau, and D. Yule, Physica D **145**, 158 (2000).
[14] Y. Timofeeva and S. Coombes, J. Math. Biol. (unpublished).
[15] J.E. Keizer and G.D. Smith, Biophys. Chem. **72**, 87 (1998).
[16] M. Falcke, L. Tsimring, and H. Levine, Phys. Rev. E **62**, 2636 (2000).
[17] L.T. Izu, W.G. Wier, and C.W. Balke, Biophys. J. **80**, 103 (2001).
[18] J.E. Keizer, G.D. Smith, S. Ponce Dawson, and J. Pearson, Biophys. J. **75**, 595 (1998).
[19] J.E. Pearson and S. Ponce Dawson, Physica A **257**, 141 (1998).
[20] J.E. Pearson, S. Ponce Dawson, J. Keizer, and G. Smith, http://www-xdiv.lanl.gov/XCM/pearson/skid/_row/_relay.ps
[21] S. Ponce Dawson, J. Keizer, and J.E. Pearson, Proc. Natl. Acad. Sci. U.S.A. **96**, 6060 (1999).
[22] S. Coombes, Bull. Math. Biol. **63**, 1 (2001).
[23] H. Hinrichsen, Adv. Phys. **49**, 815 (2000).
[24] H. Hempel, L. Schimansky-Geier, and J. Garcia-Ojalvo, Phys. Rev. Lett. **82**, 3713 (1999).
[25] B. Hu and C. Zhou, Phys. Rev. E **61**, R1001 (2000).
[26] C. Zhou, J. Kurths, and B. Hu, Phys. Rev. Lett. **87**, 098101 (2001).
[27] Color versions of all figures and animations of waves may be seen at http://www.lboro.ac.uk/departments/ma/preprints/papers03/03-02abs.html
[28] L. Meinhold and L. Schimansky-Geier, Phys. Rev. E **66**, 050901(R) (2002).
[29] J. Garcia-Ojalvo and L. Schimansky-Geier, J. Stat. Phys. **101**, 473 (2000).
[30] P. Bak, K. Chen, and M. Paczuski, Phys. Rev. Lett. **86**, 2475 (2001).
[31] M. Bär, M. Falcke, H. Levine, and L.S. Tsimring, Phys. Rev. Lett. **84**, 5664 (2000).
[32] I. Jensen, J. Phys. A **32**, 5233 (1999).
[33] P. Jung and G. Mayer-Kress, Phys. Rev. Lett. **74**, 2130 (1995).
[34] P. Jung and G. Mayer-Kress, Chaos **5**, 458 (1995).
[35] G.W. De Young and J. Keizer, Proc. Natl. Acad. Sci. U.S.A. **89**, 9895 (1992).
[36] J.W. Shuai and P. Jung, Phys. Rev. E **67**, 031905 (2003).
[37] E.A. Bugrim, A.M. Zhabotinsky, and I.R. Epstein, Biophys. J. **73**, 2897 (1997).
[38] C.S. Pencea and H.G.E. Hentschel, Phys. Rev. E **62**, 8420 (2000).
[39] J.S. Marchant and I. Parker, EMBO J. **20**, 65 (2001).
[40] M. Falcke, Biophys. J. **84**, 28 (2003).
[41] M. Falcke, Biophys. J. **84**, 42 (2003).